

## PHOTOTHERMAL SUPER RESOLUTION IMAGING: A COMPARISON OF DIFFERENT RECONSTRUCTION TECHNIQUES

**Samim Ahmadi<sup>1</sup>, Erik Thiel,  
Christina Karagianni, Philipp  
Hirsch, Mathias Ziegler**  
Bundesanstalt für  
Materialforschung und -prüfung  
(BAM)  
12200 Berlin, Germany

**Peter Burgholzer**  
RECENDT  
Research Center for  
Non-Destructive  
Testing,  
Linz, Austria

**Günther Mayr**  
Josef Ressel  
Center for Thermal  
NDE of  
Composites,  
University of  
Applied Sciences  
Upper Austria  
Wels, Austria

**Peter Jung, Giuseppe Caire**  
Technical University of Berlin  
Berlin, Department of  
Telecommunication System,  
Berlin, Germany

### ABSTRACT

*The diffusive nature of heat propagation complicates the separation of two closely spaced defects. This results in a fundamental limitation in spatial resolution. Therefore, super resolution (SR) image reconstruction can be used. SR processing techniques based on spatially structured heating and joint sparsity of the signal ensemble allows for an improved reconstruction of closely spaced defects. This new technique has been studied using a 1D laser array with randomly chosen illumination pattern.*

*This paper presents the results after applying SR algorithms such as the iterative joint sparsity (IJOSP) algorithm, to our processed measurement data. Two different data processing strategies are evaluated and discussed regarding their influence on the reconstruction goodness as well as their complexity. Moreover, the degradation of the SR reconstruction by the choice of regularization parameters in data processing is discussed*

*The application of both SR techniques that are evaluated in this paper results in a spatial resolution enhancement of approximately a factor of four which leads to a better separation of two closely spaced defects. The fundamental difference between both SR techniques is their complexity.*

Keywords: super resolution, photothermal, image reconstruction, laser array, comparison, data processing

### NOMENCLATURE

CS	Compressed Sensing
SR	Super Resolution
IJOSP	Iterative Joint Sparsity
F-SAFT	Frequency Domain Synthetic Aperture Focusing Technique
FWHM	Full Width Half Maximum

### 1. INTRODUCTION

Super resolution (SR) techniques are well-known from optics [1,2]. The SR techniques enable to enhance the spatial resolution. Inspired from this idea, scientists in fields of nondestructive testing such as photoacoustic [3] or terahertz [4] extended the scope of application. Even in fields of thermography there are first approaches [5,6].

The theory of compressed sensing (CS) is used for the realization of super resolution algorithms. CS was introduced in 2005 by Tao et al. [7]. It can be used in non-destructive testing to find the optimal solution for the reconstruction of the defects under investigation. For this purpose, an underdetermined system must be set up which can be solved by processing the measurement data with knowledge of certain system properties.

Our previous work has shown good results using an existing SR approach such as the IJOSP algorithm [6]. We adapted and applied the SR algorithm to our processed measurement data which is generated by photothermal measurements using 1D laser illumination [8,9]. This allowed to separate the closely spaced defects under investigation and therefore to enhance our spatial resolution with spatially and temporally structured heating. Since the recently obtained SR result relies on an appropriate choice of regularization parameters for the virtual wave transformation and the IJOSP algorithm [6,10], this paper presents an alternative method to make use of the IJOSP algorithm without transforming the thermal waves to virtual ultrasound waves.

<sup>1</sup> Contact author: samim.ahmadi@bam.de

## 2. MATERIALS AND METHODS

If a sample is illuminated from the front with a strongly focused laser beam, heat is generated. The heat is blurring over the depth of the sample. This fact complicates the separation of two closely spaced heat sources while measuring with the infrared (IR) camera in transmission configuration (see figure 1). The measured temperature over position diagram leads to the assumption of one heat source instead of two heat sources if the two heat sources are too close to each other.

### 2.1 Experiment

The experimental setup shown in figure 1 was used to generate the measurement data for the SR image reconstruction. The SR algorithm such as the IJOSP algorithm provides accurate results if the experiment fulfills certain conditions: sparsity, randomness [12] and the possibility to perform multiple measurements at different positions (according to MMV theory) [13]. Using this setup, a so-called “blind structured illumination” can be realized which provides randomness since the laser cells are controlled randomly in space. Further, multiple measurements with varying illumination patterns at different positions can be carried out using a National Instruments myRIO Controller that controls the linear stage as well as the random binary pattern generator. The sparsity is given due to the few slits at the sample front (designated as absorption pattern in figure 1) that are heated up only. The measurement data was generated by performing 10 measurements at 15 positions each. The measurements differ due to the randomly chosen illumination pattern. Thus, the measurement matrix contains 150 measurements.

### 2.2 Data processing

The measured temperature matrix of the IR camera in transmission configuration at  $z = L$  is designated as  $T_{meas}^i(x, y, t)$ , whereby  $i$  stands for the number of measurement and  $L$  for the thickness of the specimen. Since we are dealing with vertically oriented slits, the lateral heat flow in x-direction is of interest. For this reason, the mean is taken over the height (y-direction) so that we focus on  $T_{meas}^i(x, t)$ .

#### 2.2.1 1<sup>st</sup> reconstruction: Virtual Wave + F-SAFT

The following steps in this subsection are inspired by the data processing method of Burgholzer et al. [5].

The application of the Virtual Wave (VW) concept [10,11] enables to transform the measured thermal waves to virtual ultrasound waves  $T_{virt}^i(x, t)$ . Using an ultrasound reconstruction algorithm such as Frequency Domain Synthetic Aperture Focusing Technique (F-SAFT) enables to create a sparse basis representation of the measurements that includes an elimination of the time dimension so that a first reconstruction  $T_{rec,FSAFT}^i(x)$  is obtained.

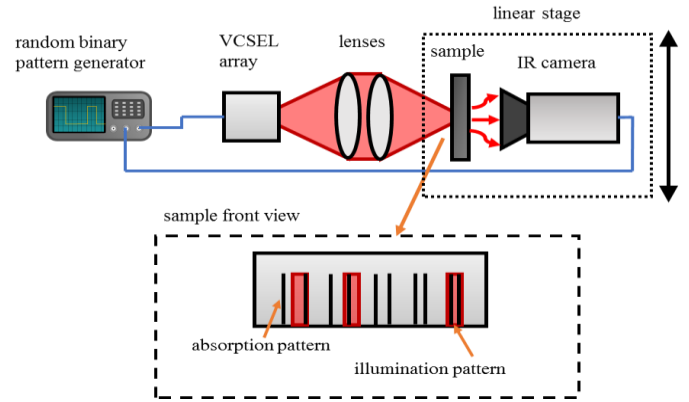


Figure 1: The sample is a 3 mm thick blackened steel sheet where aluminum foil is glued on the sample front surface. The sample front view shows an example of an illumination pattern since the VCSEL array has 12 laser lines (cells) that are controlled randomly. In this case 3 of the 12 VCSEL array cells are turned on (illumination pattern). An absorption pattern was applied to the sample surface by cutting slits into the aluminum foil. This leads to increased heating in the slit region. The absorption pattern contains 5 slit pairs with varying distances (3.0, 2.0, 1.3, 0.9, 0.6 mm). The goal is to resolve even the slit pair with the smallest distance using the IR camera in transmission configuration. For this reason, multiple measurements at different positions are done.

#### 2.2.2 1<sup>st</sup> reconstruction: Fourier transform

One standard method for conventional thermographic reconstruction is the application of the Fourier transform (FT) on the thermographic raw data. The thermographic sequence is then transformed from the time domain into the frequency domain where one can have a look at the amplitude or phase image for a certain frequency. Both transformations - VW and FT - are local transformations, which means that they are performed pixel-by-pixel.

The matrix  $T_{rec,FSAFT}^i(x)$  or  $T_{rec,Fourier}^i(x)$  depending on the choice of data processing technique is then used as input for the IJOSP routine that has already been well described [5]. The application of the IJOSP algorithm results in a matrix that is designated as  $T_{rec,IJOSP}^i(x)$  and taking the sum over  $i$  results in  $T_{rec,IJOSP}(x)$ .

## 3. RESULTS AND DISCUSSION

To emphasize the effect of using the previously described data processing steps, the diagram figure 2 compares the mean over  $i$  of  $T_{meas}^i(x, t = t_m)$  (red curve) and  $T_{rec,IJOSP}(x)$  (blue curve) whereby  $t_m$  stands for the time at which the IR camera measures the maximum temperature of the whole sequence. Figure 2 shows that each slit can be resolved. Comparing the full width half maximum (FWHM) of a red curve peak with the FWHM of a blue curve peak indicates the spatial resolution improvement. Calculating the ratio of both FWHM values results in a spatial resolution enhancement of a factor of approximately four.

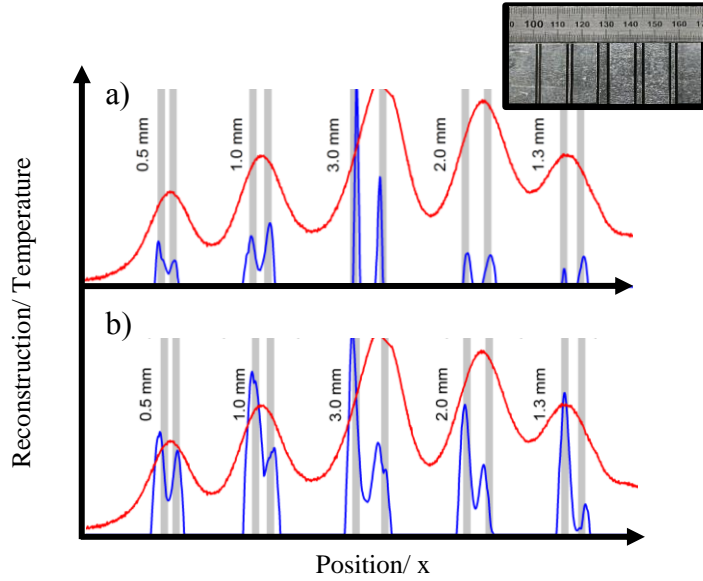


Figure 2: Reconstruction results after applying super resolution reconstruction (blue curve), mean over pixels in height and all measurements of thermographic raw data (red curve). a) VW transform + F-SAFT + IJOSP, b) Fourier Transform + IJOSP.

It should be noted that all values in the blue curve under a) 30 % and b) 20 % of the maximum amplitude (threshold value) after SR reconstruction were set to 0. This thresholding was done due to the fact that a few negligible peaks with small amplitude occur with such a large data set (150 measurements).

Furthermore, figure 2 shows that the Fourier transform can also be used to realize a sparse representation of the measurements. The solution using the Fourier transform is numerically less complex compared to the VW + F-SAFT approach. The results in terms of reconstruction quality are comparable, and it is also possible to resolve the slits using the Fourier transform and the IJOSP algorithm with the same set of measured data  $T_{meas}^i(x, t)$ . The SR reconstruction result is strongly depending on the chosen parameter set that refers to the regularization parameters that are determined manually for the IJOSP algorithm [5] as well as the regularization parameter in the VW approach [11] or the chosen frequency in the FT approach. For generating the results in figure 2 b) the amplitude images after FT were analyzed at an automatically determined frequency for each measurement  $i$ . The frequency was determined by taking into account the maximum frequency of interest  $f_m = \frac{\alpha}{\pi \mu^2}$ , whereby  $\alpha$  stands for the diffusivity and  $\mu$  for the thermal diffusion length. The frequency of interest is then determined by taking the frequency in the interval  $f = [0, f_m]$  where the amplitude image exhibits the highest SNR as well as the smallest FWHM analyzing the temperature peaks in the image.

## 4. CONCLUSION

This work has shown that the use of the IJOSP algorithm results in a spatial resolution enhancement using the VW + F-SAFT as well as the FT approach. However, it should be considered that both approaches differ in their complexity as well as in their performance and scope of application.

The VW approach can still be optimized since it relies on an inversion problem with a rank-deficient matrix where several regularization methods can be used. In addition, different ultrasound reconstruction algorithms can be applied to the virtual waves besides F-SAFT.

These optimization methods affect the sparse basis representation of the measurements and can influence the results of the SR reconstruction results. The corresponding study is part of the future work as well as studies to 2D and 3D reconstruction or measurements in reflection configuration which have not been performed yet.

## REFERENCES

- [1] Klar, T.A. *Opt. Lett.*, **24** (954), 1999
- [2] Hell, S. W. *Opt. Lett.*, **19** (780), 1994
- [3] Haltmeier, Markus. *J. Opt.*, **18** (11), 2016
- [4] Augustin, Sven. *J of IR, mm, THz waves*, **36** (17), 2015
- [5] Burgholzer, Peter. *Apl. Phys. Lett.*, **111** (031908), 2017
- [6] Burgholzer, Peter. *QIRT Journal*, submitted, 2019
- [7] Tao, Terence. *IEEE Inf Theory*, **52** (12), 2006
- [8] Thiel, Erik. *Int J Thermophys*, **40** (2), 2018
- [9] Ziegler, Mathias. *Materials Testing*, **60** (7-8), 2018
- [10] Burgholzer, Peter. *J of Apl. Phys.*, **121** (105102), 2017
- [11] Mayr, Günther. *NDT & E Intern.*, **100**, 2018
- [12] Cai, T. Tony. *Ann. Statist.*, **39** (3), 2011
- [13] Mishali, Moshe. *IEEE Sign Proc*, **57** (3), 2009